

## Portable bacterial CRISPR transcriptional activation enables metabolic engineering in *Pseudomonas putida*



Cholpisit Kiattisewee<sup>a</sup>, Chen Dong<sup>a,b</sup>, Jason Fontana<sup>a</sup>, Widiani Sugianto<sup>c</sup>, Pamela Peralta-Yahya<sup>c,d</sup>, James M. Carothers<sup>a,e,\*</sup>, Jesse G. Zalatan<sup>a,b,\*\*</sup>

<sup>a</sup> Molecular Engineering & Sciences Institute and Center for Synthetic Biology, University of Washington, Seattle, WA, 98195, USA

<sup>b</sup> Department of Chemistry, University of Washington, Seattle, WA, 98195, USA

<sup>c</sup> School of Chemistry and Biochemistry, Georgia Institute of Technology, Atlanta, GA, 30332, USA

<sup>d</sup> School of Chemical and Biomolecular Engineering, Georgia Institute of Technology, Atlanta, GA, 30332, USA

<sup>e</sup> Department of Chemical Engineering, University of Washington, Seattle, WA, 98195, USA

### ARTICLE INFO

#### Keywords:

CRISPR activation  
*Pseudomonas putida*  
Biopterin  
Mevalonate

### ABSTRACT

CRISPR-Cas transcriptional programming in bacteria is an emerging tool to regulate gene expression for metabolic pathway engineering. Here we implement CRISPR-Cas transcriptional activation (CRISPRa) in *P. putida* using a system previously developed in *E. coli*. We provide a methodology to transfer CRISPRa to a new host by first optimizing expression levels for the CRISPRa system components, and then applying rules for effective CRISPRa based on a systematic characterization of promoter features. Using this optimized system, we regulate biosynthesis in the biopterin and mevalonate pathways. We demonstrate that multiple genes can be activated simultaneously by targeting multiple promoters or by targeting a single promoter in a multi-gene operon. This work will enable new metabolic engineering strategies in *P. putida* and pave the way for CRISPR-Cas transcriptional programming in other bacterial species.

### 1. Introduction

The development of microbial platforms for industrial chemical production frequently requires optimizing the expression levels of multiple genes (Lee et al., 2019; Nielsen and Keasling, 2016). The advent of CRISPR-Cas tools that can be used to rapidly program gene expression promises to accelerate pathway engineering for the efficient production of high-value compounds (Fontana et al., 2020b). The application of CRISPR-Cas tools for transcriptional repression (CRISPRi) in bacterial metabolic engineering is well-established (Banerjee et al., 2020; Kim et al., 2019; Qi et al., 2013; Tian et al., 2019; Zheng et al., 2019). By comparison, the development of CRISPR-Cas tools for programmable transcriptional activation (CRISPRa) has lagged due to the paucity of effective transcriptional activators (Dong et al., 2018), and the complexity of the rules governing CRISPRa-directed transcription from bacterial promoters (Fontana et al., 2020a). Despite these challenges, the potential for using CRISPRa to program gene expression has been demonstrated through the successful implementation in *E. coli*, *M. xanthus*, *K. oxytoca*, and *S. enterica* (Bikard et al., 2013; Dong et al.,

2018; Ho et al., 2020; Liu et al., 2019; Peng et al., 2018). Determining how to strategically port CRISPRa systems into other microbes could significantly improve our metabolic engineering capabilities.

*Pseudomonas putida* is a gram-negative soil bacterium that has recently received attention as a potential chassis for bioproduction due to desirable metabolic capabilities and the capacity to survive harsh bioprocessing conditions (Nikel et al., 2016; Nikel and de Lorenzo, 2018) *P. putida* has high reducing power (Chavarría et al., 2013) and the ability to metabolize a broad range of feedstocks, from glucose to the toxic products of aromatic lignin degradation (Elmore et al., 2020; Johnson and Beckham, 2015; Kim et al., 2000; Loeschke and Thies, 2015). The successful implementation of CRISPR genome editing and CRISPRi in *P. putida* (Aparicio et al., 2018; Banerjee et al., 2020; Kim et al., 2019; Tan et al., 2018; Wirth et al., 2019), shows that CRISPR gene targeting can be effective in *P. putida* and provides a starting point to assess whether gene activation with a CRISPRa system can be achieved.

CRISPR-Cas transcriptional control typically uses the catalytically inactive Cas9 protein (dCas9) with programmable guide RNAs that recognize DNA targets through Watson-Crick base pairing (Xu and Qi,

\* Corresponding author. Molecular Engineering & Sciences Institute and Center for Synthetic Biology, University of Washington, Seattle, WA, 98195, USA.

\*\* Corresponding author. Molecular Engineering & Sciences Institute and Center for Synthetic Biology, University of Washington, Seattle, WA, 98195, USA.

E-mail addresses: [jcaroth@uw.edu](mailto:jcaroth@uw.edu) (J.M. Carothers), [zalatan@uw.edu](mailto:zalatan@uw.edu) (J.G. Zalatan).

2019). Recently, we identified and optimized a variant of the transcriptional activator SoxS (R93A/S101A) that can be linked to a programmable CRISPR-Cas DNA binding domain to activate gene expression in *E. coli* (Dong et al., 2018; Fontana et al., 2020a). SoxS interacts with an interface on the α-subunit of RNA polymerase (RpoA) that is widely conserved throughout bacterial species, including in *P. putida*, suggesting that the CRISPRa system we developed in *E. coli* should also be effective in *P. putida* and other bacteria. However, in contrast to the relative permissiveness of CRISPRi (and CRISPRa in eukaryotes) (Gilbert et al., 2014; Konermann et al., 2015; Qi et al., 2013), CRISPRa in bacteria is known to be sensitive to several features of target promoters, including the precise distance from the transcription start site and the intervening sequence composition. (Fontana et al., 2020a; Ho et al., 2020; Liu et al., 2019). It is not known to what extent the rules characterized in one bacterial species are generalizable in others.

In this paper, we developed CRISPRa for programming heterologous gene expression in *P. putida* KT2440. We first constructed genetic components and established experimental approaches to permit CRISPRa machinery developed in *E. coli* to be expressed and utilized in *P. putida*. By investigating promoter features that impact CRISPRa, such as guide RNA target sites and promoter strengths, we identified designs permitting 30- to 100-fold activation of heterologous reporter gene expression. We also demonstrated that CRISPRa can be coupled with CRISPRi for multi-gene programming and endogenous gene activation. Using an inducible system derived from *P. putida*, we have developed an inducible CRISPRa/CRISPRi platform with low leakage in the uninduced state. We showed that CRISPRa can drive the expression of heterologous genes to produce desirable metabolic products including biopterin derivatives and mevalonate. We further showed that the inducible CRISPRa system can generate 40-fold increases in mevalonate production, achieving titers comparable to those from a previously reported IPTG-inducible system. Taken together, this work provides a toolbox of components and validated workflows for implementing CRISPRa to program heterologous gene expression in *P. putida*. More broadly, these efforts establish a framework for the further development of CRISPRa tools for programming gene expression in industrially-promising bacteria.

## 2. Materials and methods

### 2.1. General Procedures

Plasmids pBBR1-MCS2(pBBR1-KmR), pBBR1-MCS5(pBBR1-GmR) (Kovach et al., 1995), pTNS1, pUC18T-miniTn7T-GmR (Choi and Schweizer, 2006), pRK2013, pFLP2, and *P. putida* KT2440 were a gift from the Harwood lab at the University of Washington. pRK2-AraE (Cook et al., 2018) was a gift from the Pfleger lab at the University of Wisconsin-Madison (Addgene #110141). pMVA2RBS035 (Jervis et al., 2019) was a gift from the Scrutton lab at the University of Manchester (Addgene #121051). *S. pyogenes* dCas9 (*Sp*-dCas9) was expressed from the endogenous *Sp*.*pCas9* promoter and the MCP-SoxS (R93A, S101A) (abbreviated MCP-SoxS) transcriptional activator fusion protein was expressed from the BBa\_J23107 promoter (Fontana et al., 2020a) (<http://parts.igem.org>). The modified single guide RNAs (sgRNA) (Dong et al., 2018), scaffold RNAs b2.1xMS2 (scRNAs), were expressed from the BBa\_J23119 promoter in the pBBR1-GmR plasmid, unless specified. 20 bp scRNA/sgRNA target sequences are provided in Table S4. mRFP1 and sfGFP reporters were expressed from the weak BBa\_J23117 minimal promoter (<http://parts.igem.org>), unless specified, either by integrating into the genome or in the pBBR1-GmR plasmid together with the scRNA (s). All plasmids were constructed and propagated in *E. coli* NEB turbo cells (New England Biolabs). All *P. putida* strains were constructed from the wild type strain KT2440. DNA sequences are provided in the Supplementary Material. See Table 1 for a complete list of bacterial strains and plasmid constructs.

**Table 1**  
Bacterial strains and plasmids used in this study.

Strains/Plasmids	Features	Sources
Strains		
<i>P. putida</i> KT2440	Wildtype strain	Harwood lab
PPC01	KT2440 with integrated <i>Sp</i> . <i>pCas9</i> -dCas9 and BBa_J23107-MCP-SoxS made from pPPC001	This study
PPC02	KT2440 with integrated J1-BBa_J23117-sfGFP, <i>Sp</i> . <i>pCas9</i> -dCas9, and BBa_J23107-MCP-SoxS, made from pPPC002	This study
PPC03.N	KT2440 with integrated J1(=N)-BBa_J23117-sfGFP, <i>Sp</i> . <i>pCas9</i> -dCas9, and BBa_J23107-MCP-SoxS, made from pPPC003.N	This study
PPC04	KT2440 with integrated BBa_J23111-mRFP, BBa_J1-J23117-sfGFP, <i>Sp</i> . <i>pCas9</i> -dCas9, and BBa_J23107-MCP-SoxS, made from pPPC004	This study
PPC05	PPC01 with integrated J3-BBa_J23117-mRFP and BBa_J23111-sfGFP, made from pPPC031 and pPPC032	This study
PPC06	PPC01 with integrated J3-BBa_J23117-mRFP and J3(106)-BBa_J23117-sfGFP, made from pPPC031 and pPPC033	This study
PPC07	PPC01 with integrated J3-BBa_J23117-mRFP and J3(106)-BBa_J23111-sfGFP, made from pPPC031 and pPPC034	This study
PPC08	KT2440 with integrated XylS-Pm-dCas9, BBa_J23107-MCP-SoxS made from pPPC005	This study
PPC09	KT2440 with integrated <i>Sp</i> . <i>pCas9</i> -dCas9, XylS-Pm-MCP-SoxS made from pPPC006	This study
PPC10	KT2440 with integrated XylS-Pm-dCas9, XylS-Pm-MCP-SoxS made from pPPC007	This study
Plasmids		
pUC18T-miniTn7T-Gm	Plasmid backbone for integration into <i>P. putida</i> genome, GmR/AmpR	Choi and Schweizer (2006)
pTNS1	Tn7 transposase (tnsABCD) expressing plasmid, R6K origin of replication, AmpR	Choi and Schweizer (2006)
pRK2013	Helper plasmid for triparental mating, KmR	Choi and Schweizer (2006)
pFLP2	<i>S. cerevisiae</i> Flippase expression plasmid for marker deletion, AmpR	Choi and Schweizer (2006)
pBBR1-MCS5 (pBBR1-GmR)	Broad-host-range plasmid backbone with multiple cloning site, GmR	Kovach et al. (1995)
pBBR1-MCS2 (pBBR1-KmR)	Broad-host-range plasmid backbone with multiple cloning site, KmR	Kovach et al. (1995)
pRK2-AraE	Broad-host-range plasmid backbone with AraE expressing cassette, GmR	Cook et al. (2018)
pRK2-GmR	Broad-host-range plasmid backbone with multiple cloning site, GmR	This study
pRK2-KmR	Broad-host-range plasmid backbone with multiple cloning site, KmR	This study
pGNW2	Integrative vector carrying P14g-msfGFP, KmR	Wirth et al. (2019)
pS448-CsR	CRISPR/Cas9 counterselection in Gram-negative bacteria with XylS/Pm promoter, SmR	Wirth et al. (2019)
pSEVA1213S	PRK2, PEM7-I-SceI, AmpR	Wirth et al. (2019)
pGNW2-pp1	pGNW2 derivative with integration site at prophage1, KmR	This study
pGNW2-pp2	pGNW2 derivative with integration site at prophage2, KmR	This study
pCK241	pBBR1 bearing LacI-Ptrc-mRFP, GmR	This study
pCK243	pBBR1 bearing XylS-Pm-mRFP, GmR	This study
pCK255	pBBR1 bearing I-SceI and sacB genes, GmR	This study
pMVA2RBS035	p15A, LacI-Ptrc <i>mvaE</i> , <i>mvaS</i> , <i>mvaK1</i> , <i>mvaK2</i> , and <i>mvaD</i> from <i>E. faecalis</i> , and <i>idi</i> gene from <i>E. coli</i> , KmR	Jervis et al. (2019)
pCD442		

(continued on next page)

**Table 1 (continued)**

Strains/Plasmids	Features	Sources
Strains		
pPPC001	p15A, <i>Sp.pCas9-dCas9</i> , BBa_J23107-MCP-SoxS, CmR pUC18T-miniTn7T, <i>Sp.pCas9-dCas9</i> , BBa_J23107-MCP-SoxS, AmpR/GmR	Fontana et al. (2020a) This study
pPPC002	pUC18T-miniTn7T, J1-BBa_J23117-sfGFP, <i>Sp.pCas9-dCas9</i> , and BBa_J23107-MCP-SoxS, AmpR/GmR	This study
pPPC003.N	pUC18T-miniTn7T, J1(+N)-BBa_J23117-sfGFP, <i>Sp.pCas9-dCas9</i> , and BBa_J23107_MCP-SoxS, AmpR/GmR	This study
pPPC004	pUC18T-miniTn7T, BBa_J23111-mRFP, J1-BBa_J23117-sfGFP, <i>Sp.pCas9-dCas9</i> , and BBa_J23107 MCP-SoxS, AmpR/GmR	This study
pPPC005	pUC18T-miniTn7T, XylS-Pm-dCas9, BBa_J23107-MCP-SoxS, AmpR/GmR	This study
pPPC006	pUC18T-miniTn7T, <i>Sp.pCas9-dCas9</i> , XylS-Pm-MCP-SoxS, AmpR/GmR	This study
pPPC007	pUC18T-miniTn7T, XylS-Pm-dCas9, XylS-Pm-MCP-SoxS, AmpR/GmR	This study
pPPC008	pBBR1, sgRNA or scRNA, GmR	This study
pPPC009	pBBR1, sgRNA or scRNA, KmR	This study
pPPC010	pBBR1, <i>Sp.pCas9-dCas9</i> , BBa_J23107-MCP-SoxS, scRNA, KmR	This study
pPPC011	pRK2, <i>Sp.pCas9-dCas9</i> , BBa_J23107-MCP-SoxS, KmR	This study
pPPC012	pBBR1, J1-BBa_J23117-mRFP, GmR	This study
pPPC013	pBBR1, J1-BBa_J23117-mRFP, KmR	This study
pPPC014	pRK2, J1-BBa_J23117-mRFP, GmR	This study
pPPC015	pRK2, J1-BBa_J23117-mRFP, KmR	This study
pPPC016	pBBR1, J1-BBa_J23117-mRFP, scRNA, GmR	This study
pPPC016(306)	pBBR1, J1-BBa_J23117-mRFP where J106 was replaced with J306, scRNA, GmR	This study
pPPC017	pBBR1, J1-BBa_J23117-mRFP, scRNA, KmR	This study
pPPC018	pRK2, J1-BBa_J23117-mRFP, scRNA, GmR	This study
pPPC019	pRK2, J1-BBa_J23117-mRFP, scRNA, KmR	This study
pPPC020	pBBR1, J3-BBa_J23117-mRFP, scRNA, GmR	This study
pPPC020(106)	pBBR1, J3-BBa_J23117-mRFP where J306 was replaced with J106, scRNA, GmR	This study
pPPC021.J231XX	pBBR1, J3-BBa_J231XX-mRFP, scRNA, GmR	This study
pPPC022.5 PS	pBBR1, J3-Random-5PS-BBa_J23117-mRFP, scRNA-J306, GmR	This study
pPPC023.5PSN	pBBR1, J3-Ec-5PS-BBa_J23117-mRFP, scRNA, GmR	This study
pPPC024	pBBR1, J3(106)-BBa_J23111-sfGFP, J3-BBa_J23117-mRFP, scRNA, GmR	This study
pPPC025	pBBR1, J3(106)-BBa_J23117-sfGFP, J3-BBa_J23117-mRFP, scRNA, GmR	This study
pPPC026.XN	pBBR1, PP_NNNN-mRFP, scRNA, GmR where PP_NNNN is an endogenous promoter	This study
pPPC027	pBBR1, J3-BBa_J23117-GTPCH, J3-BBa_J23117-PTPS, J3-BBa_J23117-SR, scRNA, GmR	This study
pPPC028	pBBR1, J3-BBa_J23117-GTPCH, J3-BBa_J23117-PTPS, scRNA, GmR	This study
pPPC029	pBBR1, LacI-Ptrc-mvaES, GmR	This study
pPPC030	pBBR1, J3-BBa_J23117-mvaES, scRNA, GmR	This study
pPPC031	pGNW2 derivative with integration site at prophage1 for integration of J3-BBa_J23117-mRFP cassette, KmR	This study
pPPC032	pGNW2 derivative with integration site at prophage2 for integration of BBa_J23111-sfGFP, KmR	This study
pPPC033		This study

**Table 1 (continued)**

Strains/Plasmids	Features	Sources
Strains		
pPPC034	pGNW2 derivative with integration site at prophage2 for integration of J3(106)-BBa_J23117-sfGFP, KmR	This study
	pGNW2 derivative with integration site at prophage2 for integration of J3(106)-BBa_J23111-sfGFP, KmR	

## 2.2. Plasmid construction

All PCR fragments were amplified with Phusion DNA Polymerase (Thermo-Fisher Scientific) for Infusion Cloning (Takara Bio). Transformants were cultured or selected either on Lysogeny Broth (LB) or agar plates, with appropriate antibiotics, used in the following concentrations: 100 µg/mL Carbenicillin, 25 µg/mL Chloramphenicol, 30 µg/mL Kanamycin, 30 µg/mL Gentamicin. Successful constructs were confirmed by Sanger sequencing (GENEWIZ). Details for cloning strategies are described in the [Supplementary Methods](#) and [Tables S1–S3](#). sgRNA/scRNA target sequences are provided in [Table S4](#).

## 2.3. *Pseudomonas putida* strain construction

*Pseudomonas putida* genome integrations were performed using the tri-parental conjugation for the mini-Tn7 method ([Choi and Schweizer, 2006](#)) or electroporation for the pGNW2 method ([Wirth et al., 2019](#)). Plasmid transformations into *P. putida* were performed either by electroporation ([Choi and Schweizer, 2006](#)) or heat-shock of CaCl<sub>2</sub> chemically competent cells ([Zhao et al., 2013](#)). Detailed methods for the preparation and transformation of chemically competent cells are described in the [Supplementary Methods](#).

## 2.4. Fluorescence measurements of reporter gene expression

Fluorescence measurements of reporter gene expression were carried out either by flow cytometry or plate reader. Single colonies from LB plates were inoculated in 500 µL of EZ-RDM (Teknova) supplemented with the appropriate antibiotics and grown in 96-deep-well plates at 30 °C with shaking overnight 225 rpm. For small-molecule induction, overnight cultures were diluted 100-fold into a new culture with appropriate antibiotics and inducers, then shaken overnight at 30 °C, 225 rpm. For flow cytometry, overnight cultures were diluted 1:50 in Dulbecco's phosphate-buffered saline (PBS) and analyzed on a MACS-Quant VYB flow cytometer with the MACSQuantify 2.8 software (Miltenyi Biotec) using the methods and instruments settings as described ([Dong et al., 2018](#)). For plate reader measurements, 150 µL of overnight culture were transferred into a flat, clear-bottomed black 96-well plate. OD<sub>600</sub> and fluorescence values were measured in a Bioteck Synergy HTX plate reader and analyzed using the BioTek Gen5 2.07.17 software. For mRFP1 detection, the excitation wavelength was 540 nm and emission wavelength was 600 nm. For sfGFP detection, the excitation wavelength was 485 nm and the emission wavelength was 528 nm. Data were plotted using Prism (GraphPad).

## 2.5. Mevalonate production and quantitation by GC-MS

For mevalonate production experiments, the GC-MS method was adapted from prior methods ([Pfleger et al., 2007](#)). Single colonies from LB plates were inoculated in 500 µL of EZ-RDM (Teknova) supplemented with the appropriate antibiotics and grown in 96-deep-well plates at 30 °C with shaking overnight at 225 rpm. Overnight cultures were subcultured by 1:100 dilution into 3 mL of EZ-RDM media with 1% glucose as the carbon source, supplemented with the appropriate antibiotics, and shaken at 225 rpm for 72 h at 30 °C. After 72 h, 560 µL of cell

suspension was acidified with 140  $\mu$ L of 0.5 M HCl and vortexed. 700  $\mu$ L ethyl acetate was added and samples were then vortexed again vigorously for 3 min and centrifuged at maximum speed in a benchtop centrifuge (15,000 rcf) for 10 min. The organic phase was then transferred into GC-MS vials for analysis. GC-MS analysis was performed using an Agilent 5973 instrument with a temperature program as follows. The inlet temperature was 250 °C (splitless mode). The column flow was kept at 1 mL/min in HP-5MS (Agilent). The temperature cycle started at 80 °C and was followed by a gradient of 20 °C/min to 260 °C, a second gradient of 40 °C/min to 300 °C, and a hold at 300 °C for 2 min m/z = 71, the second most abundant peak corresponding to mevalonolactone, was used for quantitation (Pfleger et al., 2007). A calibration curve was generated using freshly-prepared D,L-mevalonolactone (Sigma) dissolved in ethyl acetate. The calculated concentration was adjusted by the addition of HCl. Data were plotted using Prism (GraphPad).

## 2.6. Biopterin production and measurement

For the biopterin production experiments, single colonies from LB plates were inoculated in 500  $\mu$ L of EZ-RDM supplemented with the appropriate antibiotics and grown in 96-deep-well plates at 30 °C with shaking overnight. Each sample was then sub-cultured at 100-fold dilution in 5 mL of EZ-RDM supplemented with the appropriate antibiotics and grown in 14 mL culture tubes at 30 °C and shaking for 24 h. The overnight cultures were spun down and pteridine concentrations were determined by measuring the OD<sub>340</sub> and comparing the results to a standard calibration curve prepared with purchased reagents (Cayman Chemical). The HPLC-MS measurements were performed as described (Ehrenworth et al., 2015). A detailed HPLC-MS protocol is provided in the Supplementary Methods. Data were plotted using Prism (GraphPad).

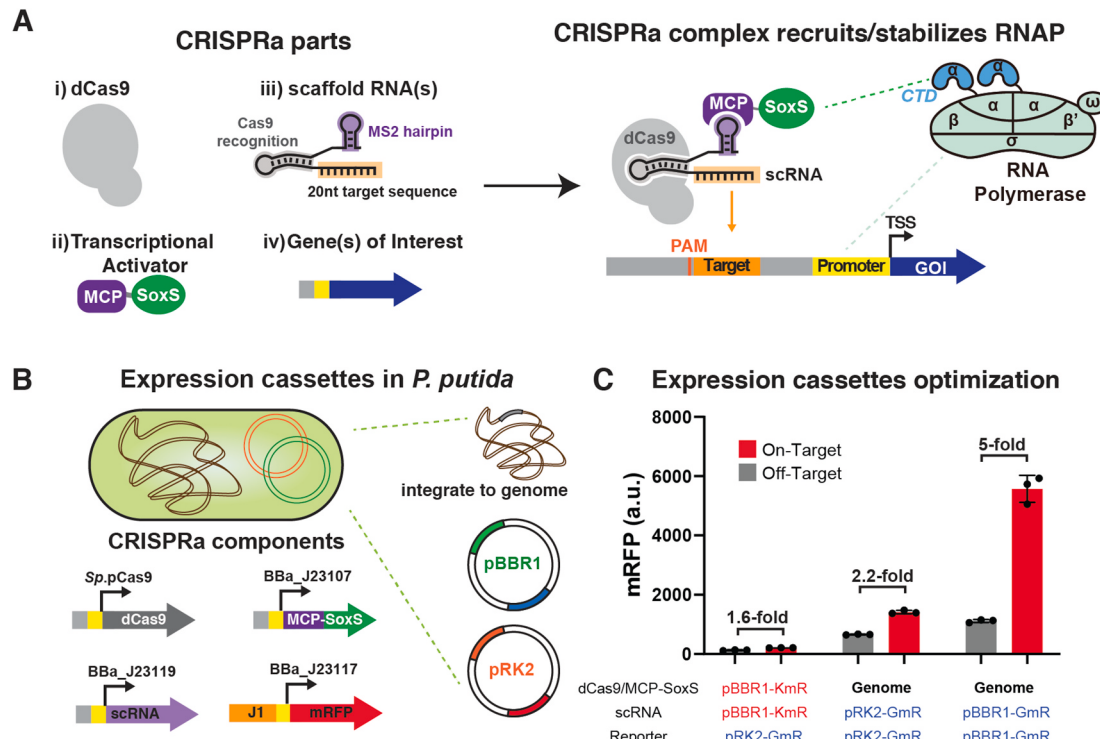


**Fig. 1.** Configuring CRISPRa in *P. putida*. (A) CRISPRa components (i-iii) are necessary to activate the gene of interest (iv). The CRISPRa ternary complex recruits and stabilizes RNA polymerase at the promoter region. (B) Available gene expression tools in *P. putida* include pBBR1 plasmid, pRK2 plasmid, and genome integration. We used two antibiotic selection markers, Gentamicin (GmR) and/or Kanamycin (KmR). (C) Testing CRISPRa in different expression systems. The CRISPRa fold-activation is highest when dCas9/MCP-SoxS were integrated into the genome and the scRNA/reporter genes were expressed on pBBR1-GmR plasmid. The J109 scRNA was used for activation and hAAVS1 was used as an off-target scRNA. Values in panel C represent the mean  $\pm$  standard deviation calculated from  $n = 3$  independent biological replicates.

genome-integrated delivery methods for the CRISPRa components. We first reduced the expression levels of dCas9 and MCP-SoxS by moving these genes from the pBBR1 plasmid to the pRK2 plasmid, which expresses transgenes at a lower level in *P. putida* (Damalas et al., 2020) (Fig. S1). This change partially mitigated the growth defect and improved the CRISPRa reporter gene expression (Fig. S2). We reduced the expression levels of dCas9 and MCP-SoxS further by integrating the dCas9/MCP-SoxS cassette into the *P. putida* KT2440 genome (generating strain PPC01). We then delivered the scRNA and reporter gene cassettes on plasmids with different combinations of two origins of replication (pBBR1 and pRK2) and two antibiotic markers (GmR and KmR) to test whether variations in the plasmid backbones impart different metabolic burdens (Mi et al., 2016). We observed the highest level of activation (~5-fold) with the scRNA and reporter both expressed from a single pBBR1-GmR backbone, while the plasmid with either pRK2 origin or KmR marker yielded weaker activation (~2-fold) (Fig. 1C and Fig. S2A). The presence of the second plasmid reduced both fold-activation by CRISPRa and basal expression of mRFP significantly (Fig. S3). In general, both CRISPRa fold-activation and the corresponding basal mRFP expression (off-target control) increased in strains that grew faster (Figs. S2 and S3), suggesting that there are different metabolic burdens associated with different delivery methods and plasmid expression systems. Taken together, these results suggest that optimizing expression levels will be important for implementing CRISPRa in new bacterial species. To improve *P. putida* CRISPRa beyond the five-fold activation obtained in Fig. 1C, we proceeded with the genetically integrated dCas9/MCP-SoxS strain (PPC01) for further optimization. While there is no specific target value for fold-activation, we aim for the largest dynamic range possible to provide the highest possible tunable range in future applications.

### 3.2. Characterization of promoter elements for optimal CRISPRa efficiency in *P. putida*

To improve the fold-activation of CRISPRa in *P. putida*, we investigated the criteria for effective CRISPRa that we previously observed in *E. coli* (Fontana et al., 2020a). Specifically, factors known to affect CRISPRa efficiency in *E. coli* include i) the distance of target sequence to transcription start-site (TSS), ii) the sequence composition of the 20 bp scRNA targeting sequence, iii) the basal minimal promoter strength, and iv) the 5'-proximal sequence composition between target sequence and minimal promoter (Fig. 2A).

#### 3.2.1. Distance to transcription start-site (TSS)

In *E. coli*, the most effective CRISPRa target sites are in the region of -60 to -100 bp before the TSS, with sharp peaks of activity every 10 bases, separated by regions of inactivity (Fontana et al., 2020a). We constructed an integrated reporter that can be targeted at multiple sites (J1-sfGFP, previously characterized in *E. coli*) (Fontana et al., 2020a) and delivered plasmids with scRNAs targeting different sites as shown in Fig. 2B. With target sites spaced 10 bp apart, the optimal sites in *P. putida* were located in the -60 to -100 bp range before the TSS, similar to that in *E. coli*. When we tested sites at single base resolution between -81 and -93 bp, we observed peaks of activity ~10–11 bases apart, similar to what we observed in *E. coli* (Fig. 2C). The efficiency of CRISPRa diminished after a 4–5 bp shift and was recovered at 10–12 bp. This finding suggests that CRISPRa has a periodic dependence on distance from the TSS, and similar effects have been observed in multiple bacterial species (Fontana et al., 2020a; Ho et al., 2020).

#### 3.2.2. scRNA target sequences

Next, we examined the 20 bp target sequence that is recognized by the scRNA. The experiments described above were performed with the J1 promoter, which contains an array of 20 base target sites. We proceeded to test an alternative promoter, termed J3, that has a different set of 20 base target sites (see Methods and Supplemental Information for

complete sequence details). We tested multiple target sites in the J3 promoter and found that the J306 site, located 81 bases upstream of the TSS, yielded the highest fold-activation (Fig. S4). Compared to the J1 promoter, where we observed 4-fold activation (J106 target site), the fold-activation with the J3 promoter increased to 34-fold (J306 target site) (Fig. 2D). For both J1 and J3, the CRISPRa-induced expression levels were similar. The large difference in fold-activation results from an unexpected difference in basal expression levels. The basal expression of J3-mRFP is 11-fold lower than that of J1-mRFP, which leads to much higher fold-activation. This difference in basal expression was not observed in *E. coli*, where J1 and J3 reporters produced 27-fold and 36-fold activation, respectively (Fontana et al., 2020a).

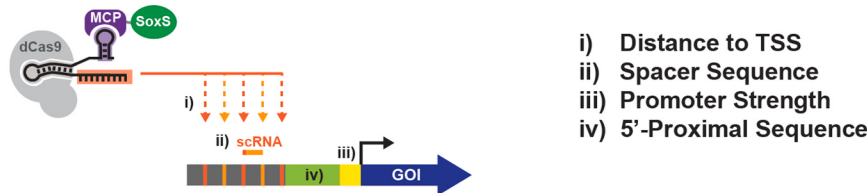
To test whether the different basal expression levels were due to differences in the 20 base target sites or to other features of the promoters, we constructed hybrid promoters where the 20 base J106 target site in J1 was replaced by J306 (J1(306)) and vice versa (J3(106)). We observed low basal expression only with the hybrid J3(106) promoter (Fig. 2D), suggesting that other sequence features of the J3 promoter besides the 20 base target site are responsible for the low basal expression of the J3 promoter. These sequence features could be upstream of the target sequence or between the target sequence and the minimal BBa\_J23117 promoter. We therefore turned our focus to the J3 upstream sequence as a basis for further optimization of CRISPRa, as it yielded the best dynamic range from the promoter sequences tested.

#### 3.2.3. Minimal promoter strength

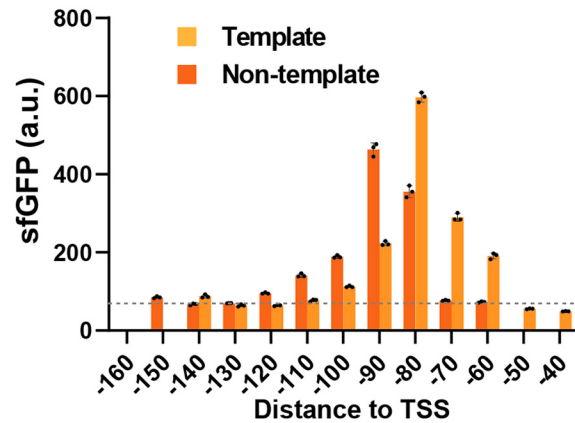
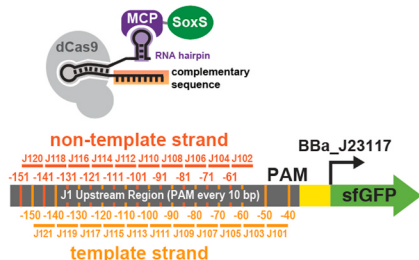
The promoters that we tested in this work consist of a 35 base minimal promoter that binds the sigma subunit of RNA polymerase and an upstream 170 base sequence region with scRNA target sites. The 35 bp minimal promoter sequence is also a key factor that governs the dynamic range of CRISPRa. In *E. coli*, we found that minimal promoter strength and the sigma factor regulating the promoter have large effects on CRISPRa (Fontana et al., 2020a). However, the alternative sigma factor regulons in *P. putida* are less characterized compared to those in *E. coli*. We therefore decided to focus on the sigma-70 regulon, the house-keeping sigma factor, that covers the majority of *E. coli* and *P. putida* endogenous promoters (Fujita et al., 1995). To test the effects of promoter strength, we introduced 11 minimal 35 base promoters from the Anderson promoter collection (BBa\_J231XX, <http://parts.igem.org>) into the J3-mRFP reporter (Fig. 3A). The variations in promoter strength arise from point mutations in the -10 and -35 sites that tune transcriptional activity; no significant changes in the transcription start sites (TSS) were detected when these promoters were experimentally characterized (Kosuri et al., 2013) (see Supplemental Information for annotated sequences).

CRISPRa-mediated expression from the Anderson promoter series followed trends similar to that previously observed in *E. coli* (Fontana et al., 2020a). When the promoter strengths are extremely weak (BBa\_J23109 and BBa\_J23113), the CRISPRa fold-activation dropped significantly to 3.1-fold and 1.4-fold compared to 27-fold with the moderately weak BBa\_J23117 minimal promoter. As promoter strength increases from BBa\_J23117 to the strong BBa\_J23110 promoter, CRISPRa fold-activation decreases because basal expression increases ~10-fold, while the maximal CRISPRa output varies by < 4-fold (Fig. 3A). CRISPRa with the strongest promoter tested (BBa\_J23111) could not be measured because no colonies were obtained when the CRISPR machinery was delivered to *P. putida* with this reporter, possibly due to the metabolic burden of expressing high levels of mRFP and the CRISPR system at the same time. The minimal BBa\_J23117 promoter yields the highest fold-activation in both *E. coli* and *P. putida* (36-fold and 27-fold, respectively) presumably because basal expression is weak enough that significant activation is possible, but not so weak that the promoter is difficult to activate. Thus, we used reporters with the BBa\_J23117 minimal promoter for further characterization and application. We note that if a higher absolute expression level is preferred, the stronger BBa\_J23106 promoter yielded the highest absolute expression

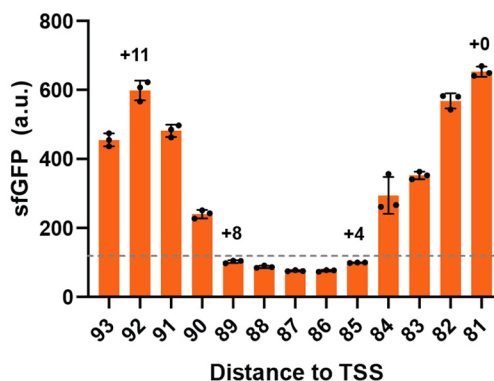
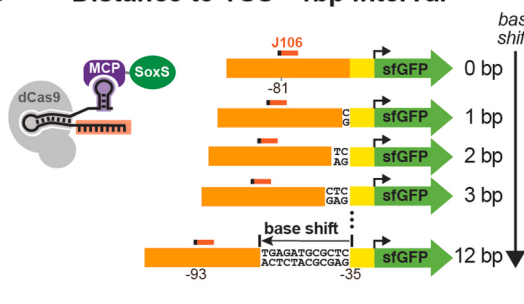
### A Factors affecting CRISPRa efficiency



### B Distance to TSS - 10bp interval



### C Distance to TSS - 1bp interval



### D scRNA sequences

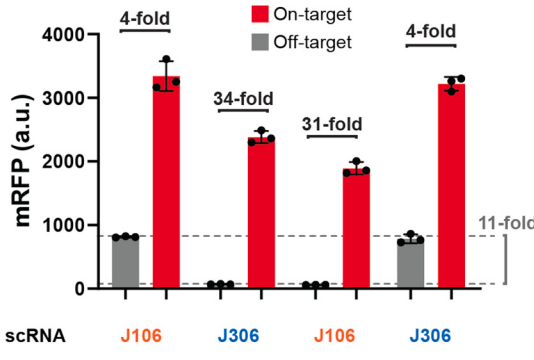
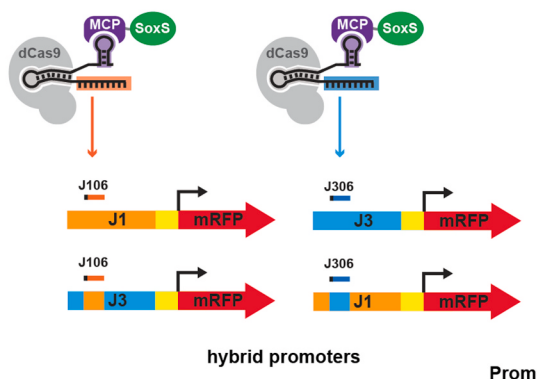


**Fig. 2. Sensitivity of CRISPRa to distance from the TSS and promoter sequence composition in *P. putida*.** (A) Factors known to affect CRISPRa efficiency in *E. coli* include i) distance to TSS, ii) scRNA target sequence, iii) minimal promoter strength, and 5'-proximal sequence between target sequence and minimal promoter. (B) Effect of distance to TSS on CRISPRa efficiency at 10 bp resolution. The J1 synthetic sequence upstream of the minimal promoter includes target sites every 10 bp in both the template strand (light orange), and the non-template strand (orange). scRNAs J101-J121 were expressed in the pBBR1-GmR backbone. The observed peaks of activation are slightly offset on the template and non-template strands because the distance is defined from the TSS to the PAM sites, which is proximal to the TSS on template strand targets and distal to the TSS on non-template strands. The most effective sites at -91 on the template strand (J108) and -80 on the non-template strand (J109) target overlapping 20-base sites. (C) Effect of distance to TSS on CRISPRa efficiency at single bp resolution. N bases were added upstream of the minimal promoter ( $N = 1-12$ ), and the J106 scRNA was used to target sites at -81 to -93 upstream of the TSS. (D) The J3 upstream sequence has lower basal expression (11-fold) and higher fold-activation by CRISPRa than the J1 sequence. When the 20 bp target sequence J306 was inserted into the J1 promoter, basal expression remains low. When the 20 bp target sequence J306 was inserted into the J3 promoter, basal expression remains high. See Methods and Supplemental Information for detailed descriptions of the J1 and J3 sequences. Values in panel B, C, and D represent the mean  $\pm$  standard deviation calculated from  $n = 3$  independent biological replicates.

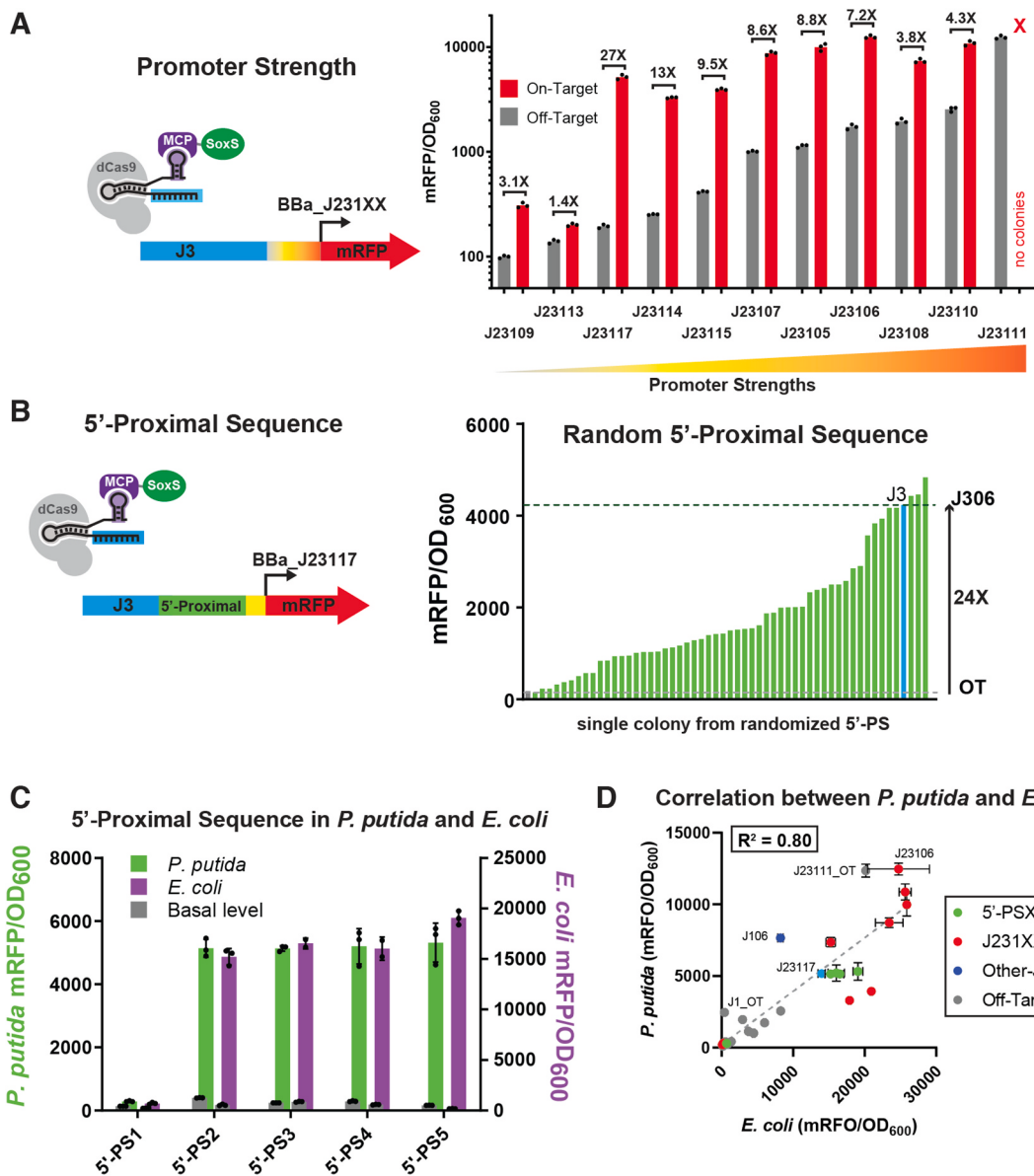


**Fig. 3.** Sensitivity of CRISPRa to promoter strength and 5' upstream sequence in *P. putida*. (A) CRISPRa is sensitive to basal promoter strength. Variants of pPPC021. J231XX were constructed by changing the BBa\_J23117 promoter into ten other minimal promoters. The promoters weaker than BBa\_J23117 exhibited low CRISPRa efficiency while the fold-activation was maximized at BBa\_J23117 and decreased as the promoter strength increased beyond that point. (B) CRISPRa is sensitive to the sequence composition of the 26 bp 5'-proximal sequence between the scRNA target site and the minimal BBa\_J23117 promoter. (C) Comparison of CRISPRa-induced expression with different 5'-proximal sequences characterized in *E. coli* and *P. putida*. Sequences are available in the Supplemental Information. (D) Correlation between CRISPRa-induced mRFP expression levels from different promoter contexts in *E. coli* and *P. putida* ( $R^2 = 0.80$ ). Values in panel A, C, D represent the mean  $\pm$  standard deviation calculated from  $n = 3$  independent biological replicates. Bars in panel B represent the value of one ( $n = 1$ ) sample.

level (2.4-fold higher than CRISPRa-mediated activation of BBa\_J23117), although the fold-activation was smaller (Fig. 3A).

#### 3.2.4. 5'-Proximal sequences

The last factor we tested is the intervening sequence between the 20 base target site and the 35 base minimal promoter, termed the 5'-proximal sequence. This sequence is 26 bp long when using an optimal target site located at -81 bp from the TSS. We constructed a pooled library of reporter gene plasmids with variable 26 base 5' proximal sequences using a randomized oligo pool (see Supplemental Methods). Each reporter retains the same 20 base J306 scRNA target site and the BBa\_J23117 minimal promoter. We transformed this library into a *P. putida* reporter strain and functionally characterized a large number of single colonies without sequencing each colony. The random 5'-proximal sequences led to a broad range of mRFP levels from CRISPRa

(Fig. 3B), similar to what we observed in *E. coli* (Fontana et al., 2020a). Random 5' proximal sequences also affect basal expression levels in the absence of CRISPRa, although these effects are relatively small (Fig. S5A). To determine if 5'-proximal sequence preferences are correlated between *E. coli* and *P. putida*, we also tested several known sequences previously characterized in *E. coli*. We observed that high-efficiency 26 bp sequences from *E. coli* yield high CRISPRa efficiency in *P. putida* while a weak sequence from *E. coli* remains weak in *P. putida* (Fig. 3C). Across the set of sequences we analyzed, one of these (5'-PS5) exhibited a higher fold activation (32-fold) compared to the J3-BBa\_J23117 promoter (27-fold). The basal expression in 5'-PS5 is 15% lower than J3-BBa\_J23117, and both sequences gave similar activated levels. We also tested whether the 26 bp 5' proximal sequence from the J1 promoter was responsible for the high basal activity of the J1 promoter (Fig. 2D). When the 26 bp 5' proximal sequence from J1

was inserted into the J3 promoter, we observed relatively low basal expression (5'-PS2 in Fig. 3C), similar to the J3 promoter. This result suggests that the 5' proximal sequence of J1 is not the cause of the high basal activity of the complete J1 promoter, and that sequence features upstream of the 5' proximal sequence and the 20 bp target site could be responsible.

The variation in CRISPRa outputs with different promoter features suggests that a set of distinct and orthogonal heterologous promoters could be developed for tunable control of gene expression. Promoters with orthogonal 20 base target sequences, together with different 5' proximal sequences, minimal promoters, and target site positions could be used to access a broad range of CRISPRa-mediated gene expression levels. Further, systematically varying the 5'-proximal sequence could allow us to identify promoters with lower basal expression and higher dynamic range of activation, similar to the case of the 5'-PS5 sequence mentioned above. We expect to be able to construct combinatorial libraries of multi-gene programs to explore how independently tuning gene expression levels in metabolic pathways affects product titers.

### 3.2.5. Correlation of CRISPRa efficiency between organisms

To compare CRISPRa in *P. putida* to that in *E. coli*, we constructed a correlation plot of mRFP expression from CRISPRa strains with different promoter sequence variations (Fig. 3D). This plot indicates that the expression level induced by CRISPRa in *E. coli* correlates well with CRISPRa in *P. putida* ( $R^2 = 0.80$ ). The fold-activation is also correlated ( $R^2 = 0.69$  Fig. S5B), although the fold-activation of *P. putida* CRISPRa tends to be lower than that of *E. coli*. The discrepancies across organisms might arise from variations in genetic context, transcription machinery, or cellular compositions between bacterial species. Despite these modest discrepancies, CRISPRa behaves largely similarly in *E. coli* and *P. putida*, suggesting that optimized CRISPRa circuits will be portable between species and that further modifications and improvements to CRISPRa systems should be readily transferable. While we do not expect these trends to be generalizable across all bacterial species, the metrics that we describe here can be systematically evaluated in alternative bacterial hosts to assess whether design principles and optimized CRISPRa circuits can be easily ported to new hosts.

### 3.3. Using *P. putida* CRISPRa for sophisticated transcriptional control strategies

With an optimized CRISPRa system in *P. putida*, we explored several strategies to enable more sophisticated control over gene expression programs. We constructed multi-gene CRISPRa/CRISPRi programs,

demonstrated endogenous gene activation, and developed an inducible CRISPRa system for tunable, dynamically-regulated expression. These strategies will enable the construction of multi-gene programs to rewire metabolic networks for optimal biosynthesis in *P. putida*.

#### 3.3.1. Multi-gene regulation by CRISPRa and CRISPRi

With optimized expression levels and a delivery strategy for the CRISPRa system in *P. putida* in place, we tested whether CRISPRa and CRISPRi can be used together to activate and repress multiple genes. This strategy has been previously successful in *E. coli* (Dong et al., 2018). We constructed a dual-reporter plasmid with weakly expressed mRFP (J3-BBa\_J23117-mRFP) and highly expressed sfGFP (J3(106)-BBa\_J23117-sfGFP). We inserted a dual scRNA/sgRNA cassette in this plasmid with a J306 scRNA for mRFP activation and an sgRNA that targets within the sfGFP open reading frame (ORF) for repression. We delivered this plasmid to a *P. putida* strain with integrated dCas9/MCP-SoxS and observed simultaneous activation of mRFP (6.6-fold) and repression of sfGFP (13-fold) (Fig. 4). The magnitude of CRISPRa fold-activation in simultaneous CRISPRa/i was weaker than the 15-fold activation that was observed if just a single scRNA was delivered to activate the mRFP reporter, possibly due to competition between multiple scRNA/sgRNA cassettes for a limited pool of dCas9.

To determine if CRISPRa can be used to activate multiple genes simultaneously, we constructed a dual-reporter plasmid with weakly expressed mRFP (J3-BBa\_J23117-mRFP) and weakly expressed sfGFP (J3(106)-BBa\_J23117-sfGFP). We inserted a dual scRNA cassette into this plasmid with scRNAs that target mRFP and sfGFP for activation and delivered it to a *P. putida* strain with integrated dCas9/MCP-SoxS. We observed simultaneous activation of mRFP (19-fold) and sfGFP (69-fold) (Fig. S6). As seen with simultaneous CRISPRa/CRISPRi, the CRISPRa effects with dual activation were weaker than those observed if each reporter was targeted individually (41-fold activation for mRFP and 105-fold activation for sfGFP), consistent with the idea that competition for dCas9 among multiple species of sgRNA/scRNA may be an issue for multi-gene programs (Huang et al., 2021). We also observed simultaneous CRISPRa at multiple genes using the weak mRFP/strong sfGFP reporter described above; the strong sfGFP could be activated a further 2-3-fold when activated by an upstream scRNA (Fig. 4).

We also demonstrated simultaneous CRISPRa/CRISPRi and dual CRISPRa on multi-gene reporters with integrated genomic reporters. The general trends were similar to what we observed with plasmid-based reporters (Figs. S7–S8), but the magnitudes of the effects were smaller, likely due to the lower copy number of the reporter gene. The ability to activate genetically-integrated heterologous reporters

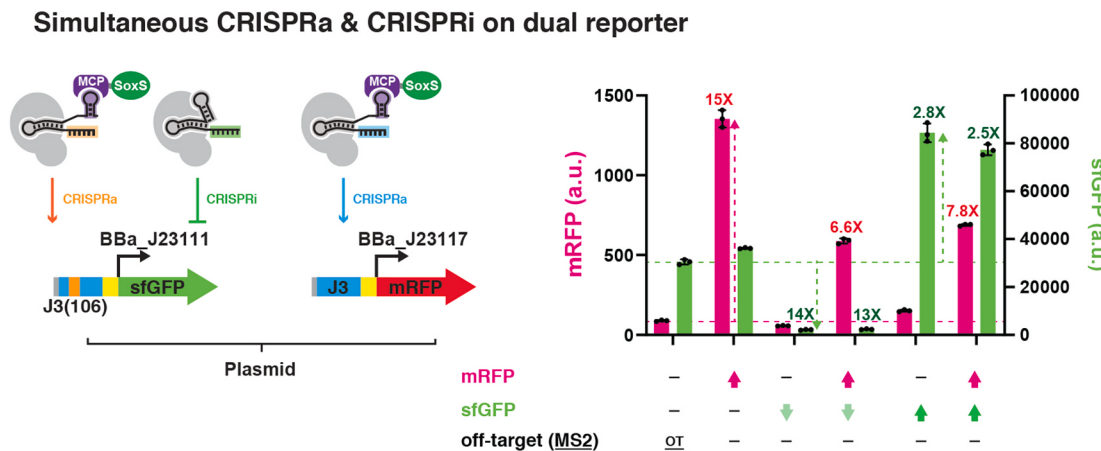


**Fig. 4. Multi-gene CRISPRa/CRISPRi in the plasmid-borne dual reporters.** A multi-gene CRISPRa/CRISPRi reporter with weakly expressed mRFP (J3-BBa\_J23117) and highly expressed sfGFP (J3(106)-BBa\_J23117) shows simultaneous activation and repression when an activator scRNA for mRFP and a repressor sgRNA for sfGFP are delivered. The strong sfGFP reporter can also be further activated ~2-3-fold if targeted by an upstream activating scRNA. This strain exhibits noticeably slower growth in both agar and liquid media (data not shown). Values represent the mean  $\pm$  standard deviation calculated from  $n = 3$  independent biological replicates.

suggests that CRISPRa may be effective at endogenous genomic targets in *P. putida*.

### 3.3.2. CRISPRa on *P. putida* endogenous promoters

To determine if CRISPRa can activate endogenous promoters, we identified a set of endogenous genes with appropriate upstream scRNA target sites. We analyzed thousands of reported TSSs for *P. putida* (D'Arrigo et al., 2016) and selected ten promoters with potentially activatable target sites located at the proper distance from the TSS. Specifically, we identified NGG protospacer adjacent motifs (PAMs), which are required for recognition of *Sp*-dCas9/guide-RNA complex (Qi et al., 2013), at distances corresponding to the J105-J112 target sites (Fig. 2B) with  $\pm 2$  bp flexibility (Fig. 2C). For each endogenous promoter, we built a reporter cassette with the promoter, flanking sequences, and an mRFP reporter gene following a strategy previously described for an *E. coli* endogenous promoter library (Zaslaver et al., 2006). We introduced on-target or off-target scRNAs into the reporter plasmid and delivered it to a *P. putida* strain with integrated dCas9/MCP-SoxS. We observed >1.5-fold activation at 4 of the 10 promoters tested, with the highest fold-activation (2.8-fold) from scRNA G2 targeting *katG* (PP\_3668) promoter (Figs. 5A and S9). The magnitudes of fold-activation from endogenous promoters are significantly lower than those under control of synthetic heterologous promoters (up to 40-fold and 100-fold for mRFP and sfGFP, respectively) (Table S5). Although higher fold-activation values may be desirable for future applications, we note that relatively modest effects can still be physiologically significant. For example, external stresses can produce a wide range of expression changes in stress-responsive genes in *P. putida*. While some changes are quite large, others are in the 2-fold to 5-fold range (Bojanović et al., 2017; Molina-Santiago et al., 2017). We suggest that tools to perturb endogenous gene expression in this range may still be effective for modulating bacterial physiology and redirecting metabolic flux. Further, we note that the ability to combine endogenous gene activation with heterologous gene activation and CRISPRi repression enables access to a vastly expanded space of gene expression programs compared to other synthetic gene regulatory methods.

This success rate and the magnitude of gene activation at endogenous targets in *P. putida* was similar to that observed previously in *E. coli* (Fontana et al., 2020a). To predictably activate any endogenous gene, we expect that it will be necessary to further elucidate the rules for effective CRISPRa. Accurate annotations of TSSs and PAM-flexible dCas9 variants to precisely target the optimal distance upstream of the endogenous gene may improve activation (Fontana et al., 2020a). Alternative bacterial activation domains are also available with different properties (Ho et al., 2020; Liu et al., 2019), and it may be possible to combine multiple activators as has been previously reported in eukaryotic systems (Chavez et al., 2015; Konermann et al., 2015).

### 3.3.3. Tunability of CRISPRa and CRISPRi with inducible promoter

To tune expression levels with CRISPRa and CRISPRi, we placed the CRISPR system components under the control of a small-molecule inducible promoter. We expressed dCas9 and/or MCP-SoxS using XylS-Pm, an inducible promoter system from the *P. putida* mt-2 toluene degradation pathway (Wirth et al., 2019). XylS-Pm provides a higher dynamic range compared to the widely-used LacI-Ptrc system (Figs. S10A and S10B). We constructed strains with inducible dCas9, inducible MCP-SoxS, or double-inducible dCas9/MCP-SoxS (PPC08-PPC10). Using a weak J3-BBa\_J23117-mRFP reporter, we induced with *m*-toluic acid (0–5 mM) and observed tunable gene activation as a function of inducer concentration in all three inducible strains (Fig. S11). This approach will enable tunable and dynamically-regulatable expression control for further applications in metabolic engineering.

Using a strong reporter (J3-BBa\_J23110-mRFP) that can be either activated or repressed, we showed that the extent of CRISPRa or CRISPRi could be tuned with different inducer levels. We delivered this reporter

with either an activating scRNA or a repressing sgRNA to the inducible dCas9 strain (PPC08) and observed 3-fold activation with CRISPRa or 7-fold repression with CRISPRi at 1 mM *m*-toluic acid (Fig. 5B). This result suggests another potential strategy for improving the dynamic range of activation from heterologous genes. By targeting CRISPRi and CRISPRa to the same locus, we may be able to obtain lower basal expression and higher induced expression. Such a strategy would require expression of only the sgRNA for repression in the off state and only the scRNA for activation in the on state, which could potentially be achieved with orthogonal induction systems or with multi-layer CRISPR circuits.

## 3.4. Metabolic engineering with CRISPRa

### 3.4.1. Biopterin pathway activation

By characterizing the promoter features necessary for effective CRISPRa in *P. putida*, we were able to apply CRISPRa for metabolic pathway engineering. We used the J3-BBa\_J23117 promoter described in the previous section to place genes of interest under the control of a CRISPRa system. In a strain with integrated dCas9/MCP-SoxS (PPC01), transcriptional units controlled by J3-BBa\_J23117 can be activated by the cognate J306 scRNA (Fig. 6A). Using this approach, we demonstrated that CRISPRa can be used to switch on two different heterologous biosynthesis pathways, one for tetrahydrobiopterin (BH4) production with multiple transcriptional units activated by the same scRNA and one for mevalonate production as a multi-gene transcriptional unit under a single promoter.

BH4 is an important cofactor in aromatic amino acid biosynthesis that can be produced from a three-enzyme pathway (Fig. 6B). BH4 has been previously produced in yeast using the *E. coli* GTPCH enzyme and the *M. alpina* PTPS and SR enzymes (Ehrenworth et al., 2015; Trenchard et al., 2015). We used the *gtpch* gene from *E. coli* MG1655 and *ptps/sr* genes from *M. alpina* that were codon-optimized for expression in *E. coli*. Each gene was placed under control of the J3-BBa\_J23117 promoter in a *P. putida* compatible plasmid (Fig. 6C). Because BH4 can be readily oxidized by atmospheric oxygen into dihydrobiopterin (BH2) and then biopterin in yeast (Ehrenworth et al., 2015), we initially screened for pathway output by absorbance at 340 nm, which reports on BH2 and biopterin. We observed a significant increase in OD<sub>340</sub> when the pathway was switched on with the cognate scRNA (Fig. 12A). Subsequent analysis by HPLC-MS to identify specific parental ions confirmed that BH2 is the major product (Fig. 6D & Fig. S12B and Fig. S13). BH2 was also detected in the off-target scRNA sample (Fig. 6D), likely due to basal expression of the biopterin pathway enzymes. When the last gene in the pathway (*sr*) was omitted, no biopterin derivatives were detected by HPLC-MS, confirming that the full pathway is necessary for heterologous biopterin production (Figs. S12A–B). Thus, biopterin pathway activation by CRISPRa was able to significantly increase heterologous production. We note that in some metabolic engineering applications, basal production may be problematic and pathway promoters may need to be modified to minimize leaky expression of the heterologous pathway genes. In future experiments, the CRISPRa system can be used to test whether product titers can be further optimized by independently activating biopterin pathway genes with orthogonal scRNAs and tuning their expression to different levels.

The major product of the biopterin pathway in *P. putida* is BH2, in contrast to *S. cerevisiae* where fully oxidized biopterin is the major product (Ehrenworth et al., 2015). The finding that BH2 is the major product suggests that the reducing potential of *P. putida* prevented BH2 from further oxidation. In *E. coli*, BH2 is the major product but the ratio of BH2:biopterin is significantly lower than in *P. putida* (Fig. S12C). Even though the fully reduced BH4, which is the desired product, was not observed in our system, the low biopterin level in *P. putida* suggests that its reducing power is advantageous for biosynthesis of oxidation-sensitive compounds.

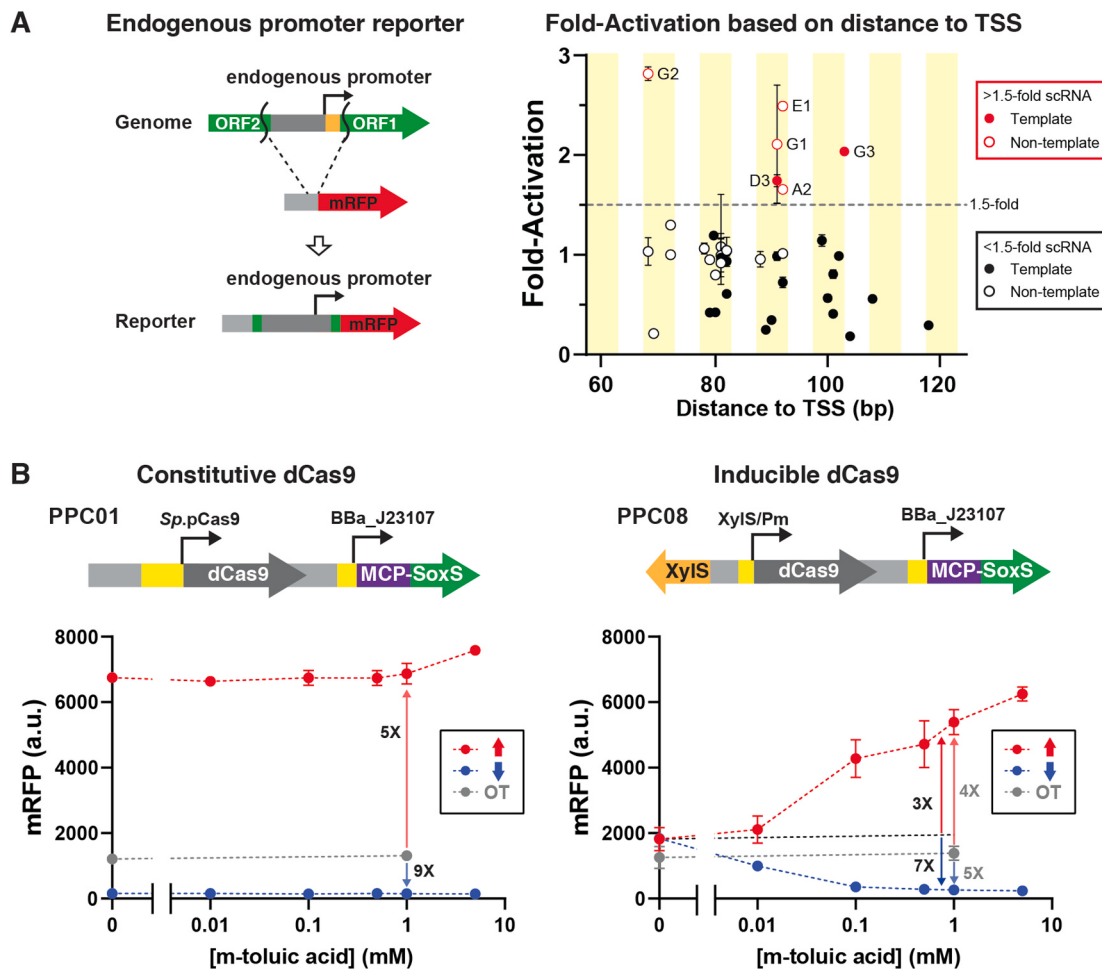


**Fig. 5. CRISPRa with endogenous promoters and inducible CRISPRa/CRISPRi in *P. putida*.** (A) The putative promoter sequences between two open reading frames (ORFs) with 60 bp flanking sequences were incorporated into the mRFP reporter. scRNAs were introduced for all potentially activatable target sites corresponding to the effective distances in Fig. 2B and C. Precise distances from the target site to the TSS are listed in Table S4. hAAVS1 was used as an off-target scRNA for all ten promoters. (B) Tunable activation of mRFP expression with CRISPRa and tunable repression of mRFP expression with CRISPRi were achieved with different inducer concentrations (0–5 mM m-toluic acid) in the inducible-dCas9 strain (right). The inducible-dCas9 strain yielded 3-fold activation with CRISPRa or 7-fold repression with CRISPRi at 1 mM m-toluic acid compared to the no-inducer control. Fold-changes compared to the off-target control were 4-fold and 5-fold, respectively. The constitutively expressed dCas9 strain (left) showed little to no response to inducer concentration. Values in panel A and B represent the mean  $\pm$  standard deviation calculated from  $n = 3$  independent biological replicates.

### 3.5. Mevalonate pathway activation

We next tested if CRISPRa could be used to produce mevalonic acid, a precursor to terpenoid natural products including fine chemicals, biofuels, and therapeutics (Anthony et al., 2009; Jervis et al., 2019; Peralta-Yahya et al., 2011). Mevalonate has previously been produced in *P. putida* using two genes, *mvaE* and *mvaS*, expressed in a single operon under the control of LacI-Ptrc (Fig. 7A) (Kim et al., 2019). We placed the *mvaES* operon under the control of J3-BBa\_J23117 synthetic promoter (Fig. 7B). The constitutively-active CRISPRa-regulated mevalonate production strain was cultured side-by-side with the LacI-Ptrc regulated *mvaES* strain as a control. We observed that the CRISPRa strain yielded  $402 \pm 21$  mg/L mevalonate, which is similar to the highest mevalonate titer of 459 mg/L obtained with LacI-Ptrc after IPTG induction (Fig. 7C). The CRISPRa-regulated *mvaES* operon enables tight control of mevalonate production, with basal mevalonate production from the off-target CRISPRa control strain indistinguishable from the empty plasmid control (Fig. 7C). In contrast, the uninduced LacI-Ptrc strain produced mevalonate levels up to  $214 \pm 57$  mg/L and yielded highly variable mevalonate levels in every IPTG concentration (ranging from 66 to 459 mg/L). We also observed highly variable IPTG-induced mRFP expression, suggesting that expression from the LacI-Ptrc promoter may be

unstable in *P. putida* (Fig. S10C). Taken together, our results demonstrate that we can effectively activate multi-gene biosynthesis pathways using a single operon (>40-fold increase in mevalonate biosynthesis, Fig. 7) or with each enzyme produced from a separate transcriptional unit with its own CRISPRa-responsive promoter (5-fold increase in BH2 production, Fig. 6).

To determine if an inducible CRISPRa system could effectively regulate mevalonate production, we tested a strain with toluid acid-inducible CRISPRa machinery (dCas9, MCP-SoxS, or both). In the absence of inducer we observed  $84 \pm 11$  mg/L mevalonate from the inducible dCas9 strain. With inducer added to this strain (0.01–1.0 mM), we observed a similar mevalonate level to that with constitutively expressed dCas9 (345–397 mg/L and  $402 \pm 21$  mg/L, respectively) (Fig. 7). The inducible MCP-SoxS strain appeared to be leaky in the absence of inducer ( $112 \pm 2$  mg/L) and gave a lower mevalonate titer when induced ( $254 \pm 9$  mg/L). The double-inducible strain, with both dCas9 and MCP-SoxS controlled by XylS-Pm, had no significant leaky production in the absence of inducer but yielded the lowest mevalonate titer ( $199 \pm 20$  mg/L). The off-target scRNA yielded a level of mevalonate indistinguishable from the empty plasmid controls (less than 10 mg/L in Fig. S14). The inducible CRISPRa system provides an additional layer of control that can be switched on at different growth phases and

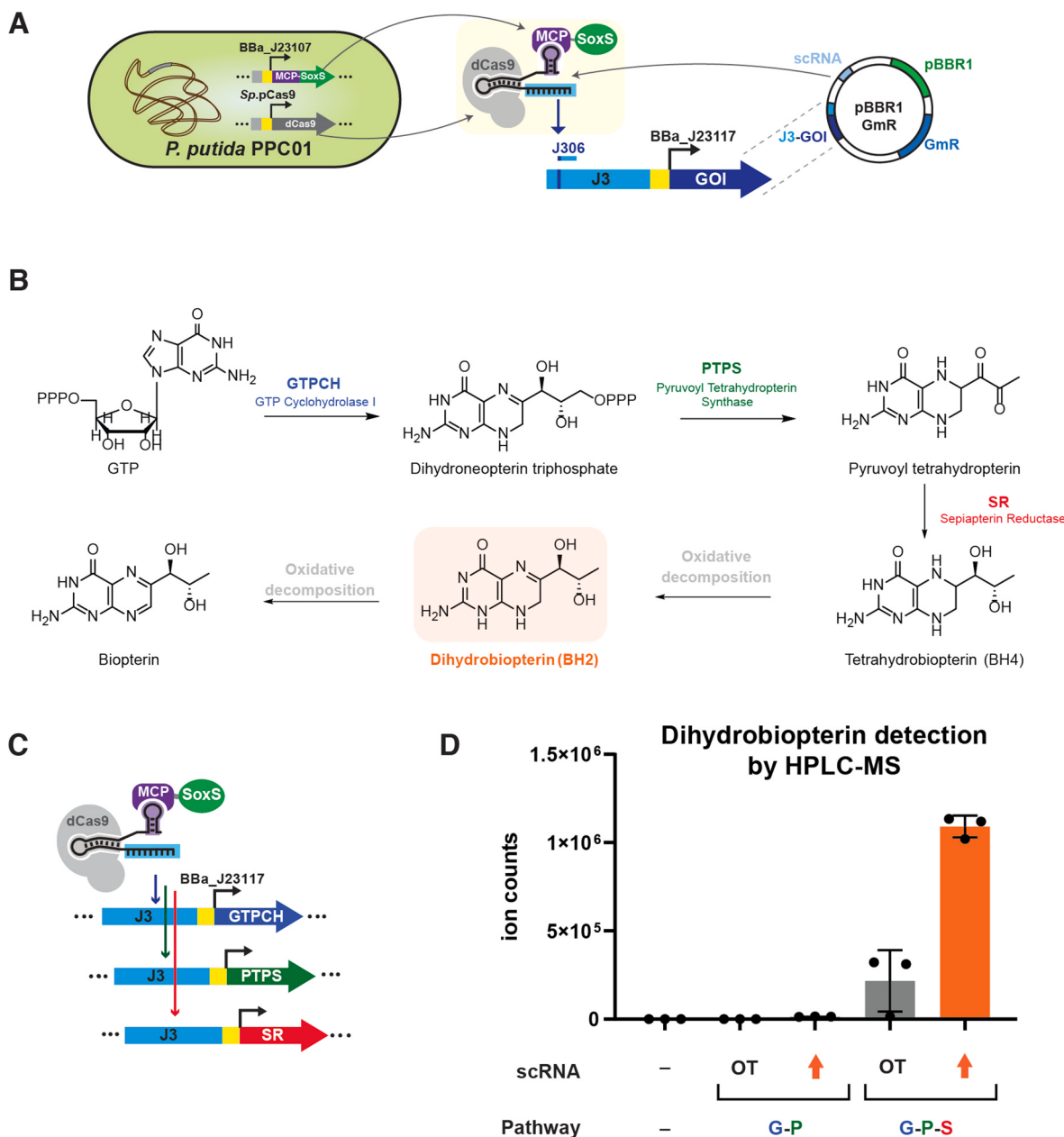


**Fig. 6. Multi-target CRISPRa activation on a biopterin pathway.** (A) Graphical depiction of CRISPRa implementation to any gene of interest by integrated dCas9/MCP-SoxS strains (PPC001) where scRNA(s) and heterologous genes were delivered on pBBR1-GmR plasmid. (B) Biosynthetic and spontaneous oxidation scheme from GTP into tetrahydrobiopterin (BH4) and its oxidized variants. The three-enzyme pathway consisted of *E. coli* *gtpch*, *M. alpina* *pps*, and *M. alpina* *sr*. Tetrahydrobiopterin is reactive towards ambient oxygen and is readily oxidized into dihydrobiopterin (BH2) and biopterin, respectively. (C) Graphical depiction of CRISPRa activating three genes with a single scRNA. (D) Dihydrobiopterin (BH2) levels observed by HPLC-MS of PPC01 strains bearing pPPC024 (3-gene pathway) or pPPC025 (absence of *sr* gene). HPLC-MS data of three biopterin species are shown in Fig. S13. Values in panel D represent the mean  $\pm$  standard deviation calculated from  $n = 3$  technical replicates.

could be coupled with an inducible CRISPRi system for multi-gene programs with both activation and repression. Compared to the LacI-Ptrc regulated *mvaES* strain, which showed significant leaky production, the inducible dCas9 CRISPRa-regulated *mvaES* strain had minimal leakage and could provide advantages in situations where leaky metabolic gene expression could be toxic or burdensome to the cell.

#### 4. Conclusions

In this work, we have ported a CRISPRa system from *E. coli* to *P. putida*. We optimized the expression methods of dCas9, MCP-SoxS, and scRNA in *P. putida* and demonstrated that the criteria for effective

CRISPRa target sites in *P. putida* are similar to that in *E. coli*. We anticipate that a similar process of optimizing expression systems will enable effective CRISPRa-regulated gene expression in a wide range of bacterial species to enable complex CRISPR-based transcriptional programming in other industrially-relevant microbes.

As reported previously in *E. coli* and in many eukaryotic systems, CRISPRa and CRISPRi can be used to target multiple genes simultaneously for activation or repression. Further, the CRISPRa system can be induced with small molecules, which will enable dynamic control of heterologous pathway activation. In *P. putida*, we applied CRISPRa to metabolic pathway engineering for tetrahydrobiopterin and mevalonate biosynthesis, providing a proof-of-concept that CRISPRa-mediated gene

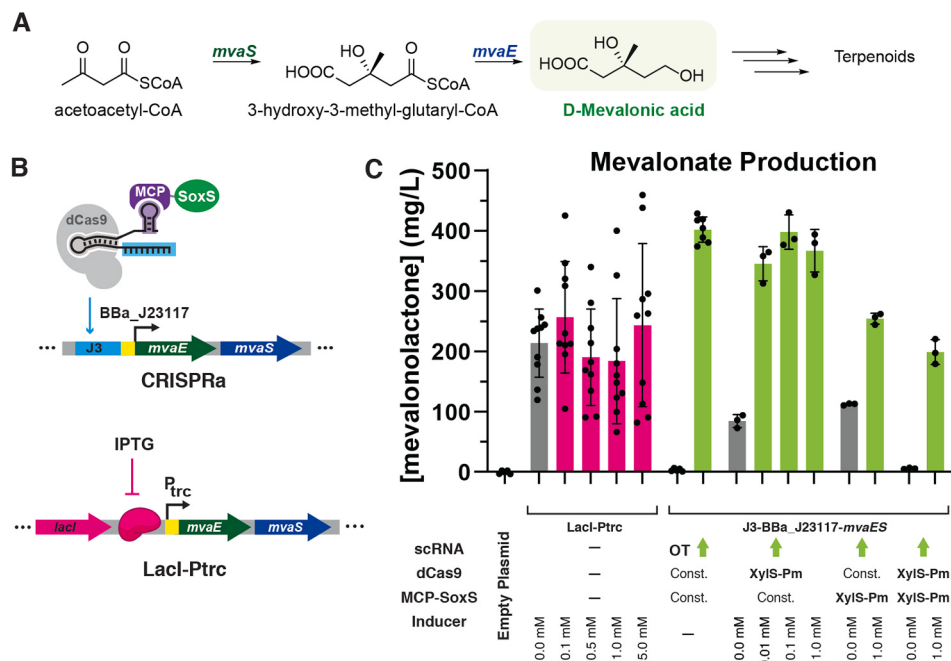


**Fig. 7. CRISPR activation on Mevalonate Production Operon.** (A) Biosynthetic pathway for D-mevalonic acid production from acetoacetyl-CoA with heterologous *mvaS* and *mvaE* genes from *Enterococcus faecalis*. (B) Graphical depiction comparing CRISPR activation complex (pPPC030) with the LacI-Ptrc inducible system (pPPC029) for gene activation. (C) Titer of mevalonate calculated based on GC-MS detection of cyclized mevalonolactone ( $m/z = 71$ ). The J306 scRNA was used as an on-target CRISPRa scRNA while hAAVS1 was used as an off-target scRNA. Up to 5.0 mM IPTG was used for induction of LacI-Ptrc and up to 1 mM m-tolulic acid was used for induction of XylS-Pm. The off-target scRNA produced a mevalonate titer indistinguishable from the no plasmid control (less than 10 mg/L, see Fig. S14). Values in panel C represent the mean  $\pm$  standard deviation calculated from  $n = 3$  independent biological replicates,  $n = 5$  for the no plasmid control and off-target scRNA,  $n = 7$  for the constitutively expressed dCas9/MCP-SoxS strain, and  $n = 10$  for the LacI-Ptrc strain.

regulation can be used to activate heterologous biosynthetic pathways.

In future work, we expect that an inducible CRISPR-Cas transcriptional control system will enable the rapid exploration of large combinatorial spaces of gene expression levels. A key advantage of CRISPR-Cas-mediated control is that, in principle, each gene of interest can be targeted by an orthogonal guide RNA and its expression level can be independently tuned. We can target endogenous genes for both activation and repression to redirect metabolic flux towards the desired pathway precursors, and we can tunably activate heterologous pathways to optimal expression levels to maximize the production of desired biosynthetic products. By learning the design principles for how to rewire metabolic networks, we expect to enable more efficient biosynthetic production pathways for valuable chemical products.

#### Declaration of competing interest

The authors declare no competing interests.

#### Acknowledgments

We thank Mary Lidstrom, Caroline Harwood, Amy Schaefer, Martin Sadilek, Luke Zhu, Nick Kruyer and members of the Zalatan, Carothers and Peralta-Yahya groups for technical assistance, advice, and helpful discussions. This work was supported by NSF Award 1817623 (J.M.C., J.G.Z.) and NSF Award 1844152 (J.M.C., P.P.Y) and DOE Award DE-EE0008927 (J.M.C., J.G.Z.).

#### Appendix A. Supplementary data

Supplementary data to this article can be found online at <https://doi.org/10.1016/j.ymben.2021.04.002>.

#### Author contributions

C.K., C.D., J.F., P.P.-Y., J.M.C., and J.G.Z. designed experiments and analyzed data. C.K., C.D., J.F., and W.S. performed experiments. C.K., C.D., J.F., J.M.C., and J.G.Z. wrote the manuscript with input from all of the authors.

#### References

- Anthony, J.R., Anthony, L.C., Nowroozi, F., Kwon, G., Newman, J.D., Keasling, J.D., 2009. Optimization of the mevalonate-based isoprenoid biosynthetic pathway in *Escherichia coli* for production of the anti-malarial drug precursor amorpho-4,11-diene. *Metab. Eng.* 11, 13–19. <https://doi.org/10.1016/j.ymben.2008.07.007>.
- Aparicio, T., de Lorenzo, V., Martínez-García, E., 2018. CRISPR/Cas9-Based counterselection boosts recombinant efficiency in *Pseudomonas putida*. *Biotechnol. J.* 13, 1700161 <https://doi.org/10.1002/biot.201700161>.
- Banerjee, D., Eng, T., Lau, A.K., Sasaki, Y., Wang, B., Chen, Y., Prahl, J.-P., Singan, V.R., Herbert, R.A., Liu, Y., Tanjore, D., Petzold, C.J., Keasling, J.D., Mukhopadhyay, A., 2020. Genome-scale metabolic rewiring improves titers rates and yields of the non-native product indigoindine at scale. *Nat. Commun.* 11, 5385. <https://doi.org/10.1038/s41467-020-19171-4>.
- Bikard, D., Jiang, W., Samai, P., Hochschild, A., Zhang, F., Marrasfiani, L.A., 2013. Programmable repression and activation of bacterial gene expression using an engineered CRISPR-Cas system. *Nucleic Acids Res.* 41, 7429–7437. <https://doi.org/10.1093/nar/gkt520>.
- Bojanović, K., D'Arrigo, I., Long, K.S., 2017. Global transcriptional responses to osmotic, oxidative, and imipenem stress conditions in *Pseudomonas putida*. *Appl. Environ. Microbiol.* 83 (7), e03236-16 <https://doi.org/10.1128/AEM.03236-16>.
- Chavarría, M., Nikel, P.I., Pérez-Pantoja, D., de Lorenzo, V., 2013. The Entner-Doudoroff pathway empowers *Pseudomonas putida* KT2440 with a high tolerance to oxidative stress. *Environ. Microbiol.* 15, 1772–1785. <https://doi.org/10.1111/1462-2920.12069>.
- Chavez, A., Scheiman, J., Vora, S., Pruitt, B.W., Tuttle, M., E, P.R.I., Lin, S., Kiani, S., Guzman, C.D., Wiegand, D.J., Ter-Ovanesyan, D., Braff, J.L., Davidsohn, N., Housden, B.E., Perrimon, N., Weiss, R., Aach, J., Collins, J.J., Church, G.M., 2015. Highly efficient Cas9-mediated transcriptional programming. *Nat. Methods* 12, 326–328. <https://doi.org/10.1038/nmeth.3312>.
- Choi, K.-H., Schweizer, H.P., 2006. mini-Tn7 insertion in bacteria with single attTn7 sites: example *Pseudomonas aeruginosa*. *Nat. Protoc.* 1, 153–161. <https://doi.org/10.1038/nprot.2006.24>.
- Cook, T.B., Rand, J.M., Nurani, W., Courtney, D.K., Liu, S.A., Pfleger, B.F., 2018. Genetic tools for reliable gene expression and recombineering in *Pseudomonas putida*. *J. Ind. Microbiol. Biotechnol.* 45, 517–527. <https://doi.org/10.1007/s10295-017-2001-5>.
- Damalas, S.G., Batianis, C., Martin-Pascual, M., de Lorenzo, V., Martins Dos Santos, V.A.P., 2020. Seva 3.1: enabling interoperability of DNA assembly among the SEVA, BioBricks and Type IIS restriction enzyme standards. *Microb. Biotechnol.* 13 (6), 1793–1806. <https://doi.org/10.1111/1751-7915.13609>.
- D'Arrigo, I., Bojanović, K., Yang, X., Holm Rau, M., Long, K.S., 2016. Genome-wide mapping of transcription start sites yields novel insights into the primary transcriptome of *Pseudomonas putida*. *Environ. Microbiol.* 18, 3466–3481. <https://doi.org/10.1111/1462-2920.13326>.
- Depardieu, F., Bikard, D., 2020. Gene silencing with CRISPRi in bacteria and optimization of dCas9 expression levels. *Methods* 172, 61–75. <https://doi.org/10.1016/j.jymeth.2019.07.024>.
- Dong, C., Fontana, J., Patel, A., Carothers, J.M., Zalatan, J.G., 2018. Synthetic CRISPR-Cas gene activators for transcriptional reprogramming in bacteria. *Nat. Commun.* 9, 2489. <https://doi.org/10.1038/s41467-018-04901-6>.

- Ehrenworth, A.M., Sarria, S., Peralta-Yahya, P., 2015. Pterin-dependent mono-oxidation for the microbial synthesis of a modified monoterpenic indole alkaloid. *ACS Synth. Biol.* 4, 1295–1307. <https://doi.org/10.1021/acssynbio.5b00025>.
- Elmore, J.R., Dexter, G.N., Salvachúa, D., O'Brien, M., Klingeman, D.M., Gorday, K., Michener, J.K., Peterson, D.J., Beckham, G.T., Guss, A.M., 2020. Engineered *Pseudomonas putida* simultaneously catabolizes five major components of corn stover lignocellulose: glucose, xylose, arabinose, p-coumaric acid, and acetic acid. *Metab. Eng.* 62, 62–71. <https://doi.org/10.1016/j.jymben.2020.08.001>.
- Fontana, J., Dong, C., Kiattisewee, C., Chavali, V.P., Tickman, B.I., Carothers, J.M., Zalatan, J.G., 2020a. Effective CRISPRa-mediated control of gene expression in bacteria must overcome strict target site requirements. *Nat. Commun.* 11, 1618. <https://doi.org/10.1038/s41467-020-15454-y>.
- Fontana, J., Sparkman-Yager, D., Zalatan, J.G., Carothers, J.M., 2020b. Challenges and opportunities with CRISPR activation in bacteria for data-driven metabolic engineering. *Curr. Opin. Biotechnol.* 64, 190–198. <https://doi.org/10.1016/j.copbio.2020.04.005>.
- Fujita, M., Hanaura, Y., Amemura, A., 1995. Analysis of the *rpoD* gene encoding the principal sigma factor of *Pseudomonas putida*. *Gene* 167, 93–98. [https://doi.org/10.1016/0378-1119\(95\)00675-3](https://doi.org/10.1016/0378-1119(95)00675-3).
- Gilbert, L.A., Horlbeck, M.A., Adamson, B., Villalta, J.E., Chen, Y., Whitehead, E.H., Guimaraes, C., Panning, B., Ploegh, H.L., Bassik, M.C., Qi, L.S., Kampmann, M., Weissman, J.S., 2014. Genome-Scale CRISPR-mediated control of gene repression and activation. *Cell* 159, 647–661. <https://doi.org/10.1016/j.cell.2014.09.029>.
- Ho, H.-I., Fang, J.R., Cheung, J., Wang, H.H., 2020. Programmable CRISPR-Cas transcriptional activation in bacteria. *Mol. Syst. Biol.* 16, e9427. <https://doi.org/10.1525/msb.20199427>.
- Huang, H.-H., Bellato, M., Qian, Y., Cárdenas, P., Pasotti, L., Magni, P., Del Vecchio, D., 2021. dCas9 regulator to neutralize competition in CRISPRi circuits. *Nat. Commun.* 12, 1692. <https://doi.org/10.1038/s41467-021-21772-6>.
- Jervis, A.J., Carbonell, P., Vinaixa, M., Dunstan, M.S., Hollywood, K.A., Robinson, C.J., Rattray, N.J.W., Yan, C., Swainston, N., Currin, A., Sung, R., Toogood, H., Taylor, S., Faulon, J.-L., Breitling, R., Takano, E., Scrutton, N.S., 2019. Machine learning of designed translational control allows predictive pathway optimization in *Escherichia coli*. *ACS Synth. Biol.* 8, 127–136. <https://doi.org/10.1021/acssynbio.8b00398>.
- Johnson, C.W., Beckham, G.T., 2015. Aromatic catabolic pathway selection for optimal production of pyruvate and lactate from lignin. *Metab. Eng.* 28, 240–247. <https://doi.org/10.1016/j.jymben.2015.01.005>.
- Kim, D.Y., Kim, Y.B., Rhee, Y.H., 2000. Evaluation of various carbon substrates for the biosynthesis of polyhydroxyalkanoates bearing functional groups by *Pseudomonas putida*. *Int. J. Biol. Macromol.* 28, 23–29. [https://doi.org/10.1016/S0141-8130\(00\)00150-1](https://doi.org/10.1016/S0141-8130(00)00150-1).
- Kim, S.K., Yoon, P.K., Kim, S.J., Woo, S.G., Rha, E., Lee, H., Yeom, S.J., Kim, H., Lee, D.H., Lee, S.G., 2019. CRISPR interference-mediated gene regulation in *Pseudomonas putida* KT2440. *Microb. Biotechnol.* 13, 210–221. <https://doi.org/10.1111/1751-7915.13382>.
- Konermann, S., Brigham, M.D., Trevino, A.E., Joung, J., Abudayyeh, O.O., Barcena, C., Hsu, P.D., Habib, N., Gootenberg, J.S., Nishimasu, H., Nureki, O., Zhang, F., 2015. Genome-scale transcriptional activation by an engineered CRISPR-Cas9 complex. *Nature* 517, 583–588. <https://doi.org/10.1038/nature14136>.
- Kosuri, S., Goodman, D.B., Cambray, G., Mutalik, V.K., Gao, Y., Arkin, A.P., Endy, D., Church, G.M., 2013. Composability of regulatory sequences controlling transcription and translation in *Escherichia coli*. *Proc. Natl. Acad. Sci. Unit. States Am.* 110, 14024. <https://doi.org/10.1073/pnas.1301301110>.
- Kovach, M.E., Elzer, P.H., Steven Hill, D., Robertson, G.T., Farris, M.A., Roop, R.M., Peterson, K.M., 1995. Four new derivatives of the broad-host-range cloning vector pBBR1MCS, carrying different antibiotic-resistance cassettes. *Gene* 166, 175–176. [https://doi.org/10.1016/0378-1119\(95\)00584-1](https://doi.org/10.1016/0378-1119(95)00584-1).
- Lee, S.Y., Kim, H.U., Chae, T.U., Cho, J.S., Kim, J.W., Shin, J.H., Kim, D.I., Ko, Y.-S., Jang, W.D., Jang, Y.-S., 2019. A comprehensive metabolic map for production of bio-based chemicals. *Nat. Catal.* 2, 18–33. <https://doi.org/10.1038/s41929-018-0212-4>.
- Lee, T.S., Krupa, R.A., Zhang, F., Hajimorad, M., Holtz, W.J., Prasad, N., Lee, S.K., Keasling, J.D., 2011. BglBrick vectors and datasheets: a synthetic biology platform for gene expression. *J. Biol. Eng.* 5, 12. <https://doi.org/10.1186/1754-1611-5-12>.
- Liu, Y., Wan, X., Wang, B., 2019. Engineered CRISPRa enables programmable eukaryote-like gene activation in bacteria. *Nat. Commun.* 10, 3693. <https://doi.org/10.1038/s41467-019-11479-0>.
- Loeschke, A., Thies, S., 2015. *Pseudomonas putida*—a versatile host for the production of natural products. *Appl. Microbiol. Biotechnol.* 99, 6197–6214. <https://doi.org/10.1007/s00253-015-6745-4>.
- Mi, J., Sydow, A., Schempf, F., Becher, D., Schewe, H., Schrader, J., Buchhaupt, M., 2016. Investigation of plasmid-induced growth defect in *Pseudomonas putida*. *J. Biotechnol.* 231, 167–173. <https://doi.org/10.1016/j.biote.2016.06.001>.
- Molina-Santiago, C., Udaondo, Z., Gómez-Lozano, M., Molin, S., Ramos, J.-L., 2017. Global transcriptional response of solvent-sensitive and solvent-tolerant *Pseudomonas putida* strains exposed to toluene. *Environ. Microbiol.* 19, 645–658. <https://doi.org/10.1111/1462-2920.13585>.
- Nielsen, J., Keasling, J.D., 2016. Engineering cellular metabolism. *Cell* 164, 1185–1197. <https://doi.org/10.1016/j.cell.2016.02.004>.
- Nikel, P.I., Chavarria, M., Danchin, A., de Lorenzo, V., 2016. From dirt to industrial applications: *Pseudomonas putida* as a Synthetic Biology chassis for hosting harsh biochemical reactions. *Curr. Opin. Chem. Biol.* 34, 20–29. <https://doi.org/10.1016/j.jcpba.2016.05.011>.
- Nikel, P.I., de Lorenzo, V., 2018. *Pseudomonas putida* as a functional chassis for industrial biocatalysis: from native biochemistry to trans-metabolism. *Metab. Eng.* 50, 142–155. <https://doi.org/10.1016/j.jymben.2018.05.005>.
- Park, W., Peña-Llopis, S., Lee, Y., Demple, B., 2006. Regulation of superoxide stress in *Pseudomonas putida* KT2440 is different from the SoxR paradigm in *Escherichia coli*. *Biochem. Biophys. Res. Commun.* 341, 51–56. <https://doi.org/10.1016/j.bbrc.2005.12.142>.
- Peng, R., Wang, Y., Feng, W., Yue, X., Chen, J., Hu, X., Li, Z., Sheng, D., Zhang, Y., Li, Y., 2018. CRISPR/dCas9-mediated transcriptional improvement of the biosynthetic gene cluster for the epothilone production in *Myxococcus xanthus*. *Microb. Cell Fact.* 17, 15. <https://doi.org/10.1186/s12934-018-0867-1>.
- Peralta-Yahya, P.P., Ouillet, M., Chan, R., Mukhopadhyay, A., Keasling, J.D., Lee, T.S., 2011. Identification and microbial production of a terpene-based advanced biofuel. *Nat. Commun.* 2, 483. <https://doi.org/10.1038/ncomms1494>.
- Pfleger, B.F., Pitera, D.J., Newman, J.D., Martin, V.J.J., Keasling, J.D., 2007. Microbial sensors for small molecules: development of a mevalonate biosensor. *Metab. Eng.* 9, 30–38. <https://doi.org/10.1016/j.jymben.2006.08.002>.
- Qi, L.S., Larson, M.H., Gilbert, L.A., Doudna, J.A., Weissman, J.S., Arkin, A.P., Lim, W.A., 2013. Repurposing CRISPR as an RNA-guided platform for sequence-specific control of gene expression. *Cell* 152, 1173–1183. <https://doi.org/10.1016/j.cell.2013.02.022>.
- Shetty, R.P., Endy, D., Knight, T.F., 2008. Engineering BioBrick vectors from BioBrick parts. *J. Biol. Eng.* 2, 5. <https://doi.org/10.1186/1754-1611-2-5>.
- Tan, S.Z., Reisch, C.R., Prather, K.L.J., 2018. A robust CRISPR interference gene repression system in *Pseudomonas*. *J. Bacteriol.* 200 <https://doi.org/10.1128/jb.00575-17>.
- Tian, T., Kang, J.W., Kang, A., Lee, T.S., 2019. Redirecting metabolic flux via combinatorial multiplex CRISPRi-mediated repression for isopenetol production in *Escherichia coli*. *ACS Synth. Biol.* 8, 391–402. <https://doi.org/10.1021/acssynbio.8b00429>.
- Trenchard, I.J., Siddiqui, M.S., Thodey, K., Smolke, C.D., 2015. De novo production of the key branch point benzylisoquinoline alkaloid reticuline in yeast. *Metab. Eng.* 31, 74–83. <https://doi.org/10.1016/j.jymben.2015.06.010>.
- Wirth, N.T., Kozaeva, E., Nikel, P.I., 2019. Accelerated genome engineering of *Pseudomonas putida* by I-SceI-mediated recombination and CRISPR-Cas9 counterselection. *Microb. Biotechnol.* 13, 233–249. <https://doi.org/10.1111/1751-7915.13396>.
- Xu, X., Qi, L.S., 2019. A CRISPR-dCas toolbox for genetic engineering and synthetic biology. *J. Mol. Biol.* 431, 34–47. <https://doi.org/10.1016/j.jmb.2018.06.037>.
- Zaslaver, A., Bren, A., Ronen, M., Itzkovitz, S., Kikoin, I., Shavit, S., Liebermeister, W., Surette, M.G., Alon, U., 2006. A comprehensive library of fluorescent transcriptional reporters for *Escherichia coli*. *Nat. Methods* 3, 623–628. <https://doi.org/10.1038/nmeth895>.
- Zhang, S., Voigt, C.A., 2018. Engineered dCas9 with reduced toxicity in bacteria: implications for genetic circuit design. *Nucleic Acids Res.* 46, 11115–11125. <https://doi.org/10.1093/nar/gky884>.
- Zhao, F., Zhang, Y., Li, H., Shi, R.J., Han, S.Q., 2013. [CaCl<sub>2</sub>-heat shock preparation of competent cells of three *Pseudomonas* strains and related transformation conditions]. *Yingyong Shengtai Xuebao* 24, 788–794.
- Zheng, Y., Su, T., Qi, Q., 2019. Microbial CRISPRi and CRISPRa systems for metabolic engineering. *Biotechnol. Bioproc. Eng.* 24, 579–591. <https://doi.org/10.1007/s12257-019-0107-5>.